Paper # 070IC-0003 **Topic: Internal Combustion and Gas Turbine Engines**

8^{th} US National Combustion Meeting
Organized by the Western States Section of the Combustion Institute
and hosted by the University of Utah
May 19-22, 2013.

Computational Study of Partial Fuel Stratification for HCCI Engines Using Gasoline Surrogate Reduced Mechanism

Benjamin Wolk *Jyh-Yuan Chen*

Department of Mechanical Engineering,
University of California-Berkeley, Berkeley, CA, USA 94720

Fuel stratification is a potential strategy for reducing the maximum pressure rise rate in HCCI engines. Simulations of Partial Fuel Stratification (PFS) have been performed using a modified version of KIVA-3V that computes chemistry using CHEMKIN. A 96-species reduced mechanism for a 4-component gasoline surrogate has been developed from a 312-species skeletal mechanism given by Mehl, et al. (2011) using the Computer Assisted Reduction Mechanism algorithm (the detailed mechanism from Lawrence Livermore National Laboratory has about 1400 species and 6000 reactions). The reduced mechanism is validated for ignition delay against the detailed mechanism and experimental shock tube data. Simulations of PFS and HCCI engine operation using the gasoline surrogate and PRF73 were performed for a CFR engine of compression ratio 14:1 at ambient and boosted intake pressures. The temperature distribution of the mixture stratification dictates whether single-stage or multi-stage combustion is observed for PFS. For the gasoline surrogate at an intake pressure of 2 bar, PFS results in multi-stage combustion because the increased low temperature heat release leads to thermal equilibration among the different equivalence ratio regions such that the richer regions auto-ignite prior to the lean regions. At ambient intake pressure, the absence of low temperature heat release leads to thermal stratification that offsets the differences in ignition delay among the equivalence ratio regions, resulting in single-stage combustion. For PRF73 at ambient conditions, PFS results in multi-stage combustion for sufficiently late injection timing for which low temperature heat release is observed.

1 Introduction

In order to limit carbon dioxide and pollutant emissions from internal combustion (IC) engines, next-generation low-temperature compression ignition (CI) combustion modes that reduce exhaust emissions and improve thermal efficiency are currently being explored. The advanced low-temperature combustion (LTC) modes receiving substantial research attention include Homogeneous Charge Compression Ignition (HCCI), Spark-Assisted Compression Ignition (SACI), Stratified Charge Compression Ignition (SCCI), and Reactivity Controlled Compression Ignition (RCCI). Both HCCI and SACI use homogenous fuel-air mixtures and rely on fuel auto-ignition characteristics for combustion phasing, although SACI has the advantage of spark ignition to influence the start of combustion (SOC). At high loads, extremely rapid combustion can occur leading to knock (pressure oscillations) and, ultimately, engine damage. HCCI and SACI must use lean fuel-air mixtures or high levels of exhaust gas recirculation (EGR) to lower the heat release rate (HRR) such that the maximum pressure rise rate (PRR_{max}) is acceptable [1]. Although homogeneous fuel mixtures are targeted in HCCI combustion, thermal stratification has been shown to play an

important role in dictating HRR and PRR_{max} [2–4]. Fuel stratification has also been shown to influence HRR and PRR_{max} [5–9].

SCCI aims to reduce PRR_{max} by using Partial Fuel Stratification (PFS) to prolong combustion [5–9] and enable engine operation at high load conditions. PFS is accomplished by mixing the majority of the fuel with intake air and direct-injecting (DI) the rest during the compression stroke. The goal of preparing a stratified mixture is to promote sequential auto-ignition that reduces PRR_{max}. RCCI is similar to SCCI in that gradients in reactivity are introduced to promote sequential auto-ignition, however, RCCI uses two or more fuels of varying reactivity introduced in seperate injection events [10]. The fuel auto-ignition chemistry is critical in SCCI and the behavior of PFS depends on how the auto-ignition characteristics of the fuel (or fuel-blend) change with equivalence ratio (ϕ) and if the fuel exhibits single- or multi-stage ignition [6].

The ϕ-sensitivity of a fuel describes how its auto-ignition characteristics change with ϕ and is an indicator of how a fuel will respond to stratification [5–7]. A fuel is considered ϕ-sensitive if increasing ϕ advances the HCCI combustion phasing. For gasoline at ambient intake pressure, increasing ϕ delays the hot-ignition (thermal-runaway) timing because the reduced ratio of specific heats ($\gamma = c_p/c_v$) decreases the compressed-gas temperature. Thus, gasoline is not ϕ-sensitive at ambient intake conditions. Conversely, PRF73 is ϕ-sensitive at ambient intake conditions; increasing ϕ advances the hot-ignition timing because the heat released from pre-ignition reactions increases with ϕ and compensates for the reduced γ. Gasoline becomes ϕ-sensitive at boosted intake conditions because the pre-ignition reactions become more active at increased pressure and are more prominent for larger ϕ. PFS is expected to result in multi-stage ignition for ϕ-sensitive fuels where the heat released from pre-ignition reactions increases with ϕ.

In addition to experimental investigations, computer simulations have been performed for stratified-charge engine operation [11, 12]. In [11], the effects of swirl, injection pressure, injector hole-size, number of injector holes, injection timing, and piston geometry on mixture stratification of non-reacting iso-octane/air mixtures were investigated. Injection timing was found to be the most important factor influencing mixture stratification with the other factors having secondary, although distinct, effects. In [12], fully coupled multi-dimensional computational fluid dynamics (CFD) and chemical kinetics simulations of n-heptane/air mixture stratification and combustion were conducted using a 42-species reduced mechanism [13] for a naturally aspirated engine. Evaporative cooling from the fuel injection decreased the temperature of the richer regions, such that only the lean premixed charge unaffected by the spray released heat at low temperatures (~780 K). After the low temperature reactions, the in-cylinder temperature was almost uniform and hot ignition occurred first in the richer regions. Changes in the emission of carbon monoxide (CO), nitrogen oxides (NO_x), and unburnt hydrocarbons (UHC) with stratification are also discussed in [12].

In a review of CI engines, Dec [2] notes that CI engine modeling requires improved chemical-kinetic models that more accurately predict low temperature heat release (LTHR), pressure-boost effects, and the behavior of realistic fuels. Accurate prediction of LTHR is important because LTHR influences the chemistry leading up to hot ignition [14]. Additionally, the higher temperature rise rate prior to hot ignition resulting from LTHR reduces the influence of random fluctuations in the charge temperature on the hot ignition timing [15]. Accurately predicting the effects of pressure-boost is important because the LTHR characteristics of a fuel can change with pressure (e.g. gasoline).

In this work, a 96-species reduced mechanism for a 4-component gasoline surrogate has been developed for CI engine simulations. Fully coupled CFD and chemical kinetics simulations are conducted to further investigate observations from [5] that the reduction of PRR_{max} using PFS is intake pressure (P_{in}) dependent for gasoline-fueled engines. Specifically, the experimental observations that PFS leads to multi-stage combustion at P_{in} = 2 bar and single-stage combustion at P_{in} = 1 bar will be investigated. Additionally, the experimental observation from [6] that PFS with PRF73 results in multi-stage combustion for sufficiently late injection timing at P_{in} = 1 bar is investigated.

2 Reduced Mechanism Development and Validation

A 96-species reduced mechanism for a 4-component gasoline surrogate was developed from a 312-species skeletal mechanism given in [16] using the Computer Assisted Reduction Mechanism (CARM) algorithm [17]. The 96-species reduced mechanism is comprised of 92 reactions and 209 quasi-steady-state (QSS) species. The skeletal mechanism includes about 1500 reactions and was derived from a detailed mechanism [18] from LLNL (Lawrence Livermore National Laboratory) with about 1400 species and 6000 reactions.

In the CARM algorithm, QSS species are identified by evaluating their concentration levels and with the help of a rate-of-production analysis. After selection of the QSS species, a set of independent elementary reaction steps is chosen to eliminate the QSS species in order to permit systematic construction of the reduced mechanism. Algebraic expressions for the QSS species are obtained in terms of the concentrations of the major species such that the QSS species can be solved for numerically, as they are non-linearly coupled. CARM evaluates choices made for mechanism reduction by comparing CHEMKIN [19] flame code (e.g. SENKIN, PREMIX, ect.) results using the newly developed reduced mechanism to those of the detailed mechanism. If the choice of QSS species leads to agreement of flame code results between the newly reduced and detailed mechanisms (within 10% for the current study), the mechanism is saved and further refinement can be attempted in the subsequent iteration. Conversely, if there is not agreement between the newly developed reduced mechanism and the detailed one, the choice of QSS species is attempted again using the previous successful iteration of the reduced mechanism.

The current mechanism was reduced using the target conditions for auto-ignition delay (t_{ign}) presented in Table 1. The target conditions span lean to rich mixtures at pressures and temperatures characteristic of boosted CI engine operation. Flame speed target conditions were not considered for the current mechanism reduction, however, flame speed was considered for the development of the skeletal mechanism. Futher refinement of the reduced mechanism could incorporate flame speed targets, although the size of the mechanism would likely increase. Consideration of flame speed target conditions could be important for mechanisms used in simulations of SACI and SI engine operation where flame propagation is important.

The reduced mechanism has been validated for auto-ignition by comparing SENKIN simulations with the reduced mechanism against SENKIN simulations with the detailed mechanism and experimental shock tube data [20]. Table 2 summarizes the current gasoline surrogate (from [16]) and the gasoline and gasoline surrogates used in [20]. Figures 1 and 2 compare auto-ignition delay times from simulations and experiments for ϕ = 1.0 (0% EGR) and ϕ = 0.5 (0% EGR),

Table 1: CARM Target Conditions

Condition	ϕ	T [K]	P [bar]	Condition	ϕ	T [K]	P [bar]
1	0.2	750	10	7	0.6	1000	60
2	0.2	750	80	8	1.0	800	10
3	0.3	800	40	9	1.0	750	60
4	0.6	800	10	10	2.0	1100	10
5	0.6	1100	10	11	2.0	700	20
6	0.6	750	60	12	2.0	800	40

respectively, at 20 atm and 55 atm. Figures 3 and 4 compare auto-ignition delay times from simulations and experiments for ϕ = 2.0 (0% EGR) and ϕ = 0.5 (20% EGR), respectively, at 20 atm and 55 atm. There is good agreement between the experimental values and those calculated using SENKIN with the reduced mechanism. The reduced mechanism also shows good agreement with the detailed mechanism.

As a simple illustration of the computational speedup provided by the reduced mechanism, consider an auto-ignition delay calculation using SENKIN for ϕ = 1.0, T = 1000 K, P = 20 atm, and 0% EGR. Using a single processor, the detailed mechanism requires 9 minutes 44 seconds, the skeletal mechanism requires 27.41 seconds, and the reduced mechanism requires 3.64 seconds. The reduced mechanism provides ~160x speed up compared to the detailed mechanism and ~7.5x speedup compared to the skeletal mechanism. The computational speedup provided by the reduced mechanism is important for use in coupled CFD and chemical kinetic codes for large scale simulations, such as IC engine combustion.

Comparisons of laminar flame speeds simulated with CHEMKIN using the reduced mechanism to those simulated with the detailed mechanism [16] and to experiments [21, 22] are presented in the appendix.

Table 2: Gasoline and Gasoline Surrogates

Fuel	iC_8H_{18}	nC_7H_{16}	$C_6H_5CH_3$	$C_5H_{10}-2$	Ref.
Current Surrogate	57%	16%	23%	4%	[16]
Surrogate A	63%	17%	20%	0%	[20]
Surrogate B	69%	17%	14%	0%	[20]
RD387 Gasoline	Many components; (RON+MON)/2 = 87				[20]

3 KIVA-3V/CHEMKIN

KIVA-3V [23] is a CFD code that uses an arbitrary Lagrangian-Eulerian method to simultaneously solve the Navier-Stokes equations and liquid spray droplet dynamics. The current version of KIVA-3V has been modified to compute chemistry using CHEMKIN. The standard k-ϵ turbulence model is used and droplet breakup is predicted using the Kelvin-Helmholtz Raleigh-Taylor (KHRT) breakup model [24]. Simulations were performed using a Cooperative Fuel Research (CFR) engine of compression ratio (CR) 14:1. This is the same compression ratio as [5] and [6], however, the engine displacement is smaller in this work and a flat piston is used. Additionally, the

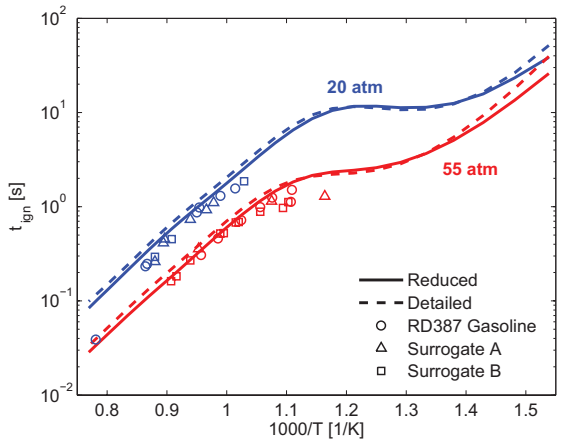

Figure 1: Auto-ignition delay times for ϕ = 1.0, 0% EGR from simulation and experiments show good agreement. The reduced mechanism shows good agreement with the detailed mechanism.

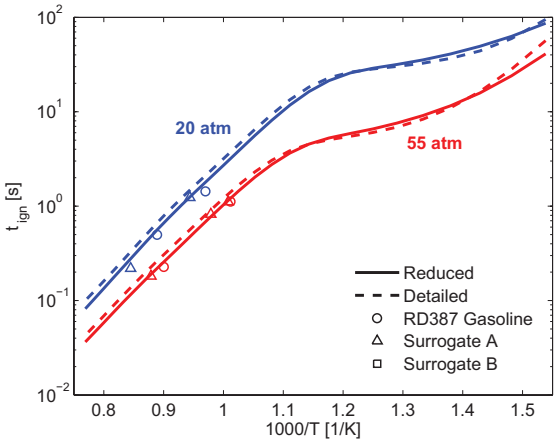

Figure 2: Auto-ignition delay times for ϕ = 0.5, 0% EGR from simulation and experiments show good agreement. The reduced mechanism shows good agreement with the detailed mechanism.

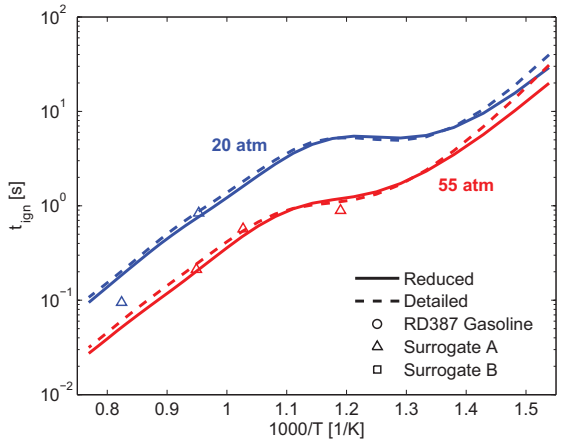

Figure 3: Auto-ignition delay times for ϕ = 2.0, 0% EGR from simulation and experiments show good agreement. The reduced mechanism shows good agreement with the detailed mechanism.

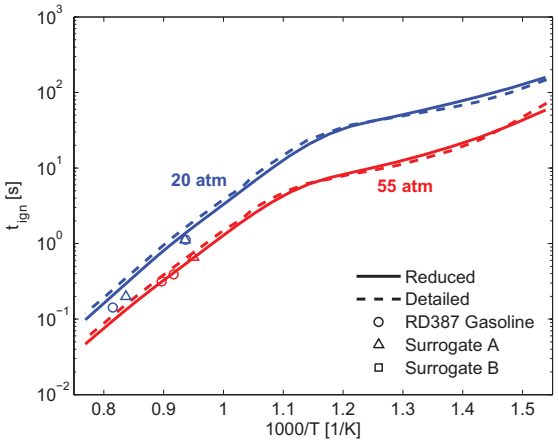

Figure 4: Auto-ignition delay times for ϕ = 0.5, 20% EGR from simulation and experiments show good agreement. The reduced mechanism shows good agreement with the detailed mechanism.

current work employs a single-hole injector as opposed to an 8-hole injector in [5] and [6]. The current single-hole injector has a spray cone angle of 60° (included angle of 30°), a spray cone thickness of 10°, Sauter Mean Diameter (SMD) of 80 µm, 120 m/s injection velocity, and initial droplet temperature of 300.15 K. Engine parameters are summarized in Table 3. The structured computational grid is shown in Fig. 5 with 33,500 grid points at 290 CAD, which reduces to 16,300 grid points at top-dead center (TDC) ($TDC_{compression}$ = 360 CAD).

Table 3: CFR Engine Parameters

Displacement	0.616 L
Stroke	114.3 mm
Bore	82.25 mm
Connecting rod	254 mm
Squish	9.557 mm
Compression ratio	14:1 (variable)
Number of valves	2
Engine speed	1200 rpm
Intake valve opening	17 CAD
Intake valve closure	207 CAD
Exhaust valve opening	508 CAD
Exhaust valve closure	7 CAD

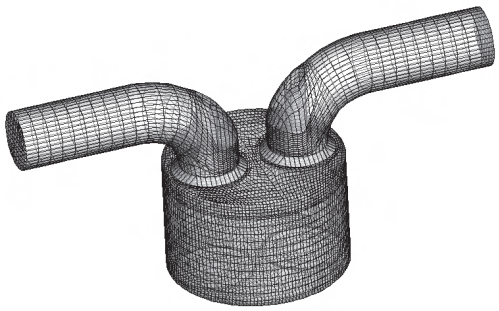

Figure 5: Computational grid of CFR engine at 290 CAD.

4 Results and Discussion

4.1 Gasoline Surrogate

Simulations were performed for HCCI and PFS engine operation at boosted and ambient intake conditions. HCCI operation was accomplished using an equivalence ratio of ϕ = 0.35 with 7.8% EGR determined using a single zone well-mixed reactor code. PFS operation was accomplished using a homogenous mixture of ϕ = 0.30 (7.8% EGR) with the remaining fuel direct injected at a start of injection (SOI) of 310 CAD or 330 CAD to achieve a global ϕ = 0.35 (15% DI). The intake temperature (T_{in}) was chosen such that the earliest combustion phasing was near TDC. For P_{in} = 2 bar, T_{in} = 370 K and for P_{in} = 1 bar, T_{in} = 420 K.

The in-cylinder pressure and HRR from chemical reactions determined from simulations are presented in Figs. 6 and 7 for P_{in} = 2 bar and Figs. 8 and 9 for P_{in} = 1 bar. The insets of Figs. 7 and 9 highlight the LTHR range prior to the main combustion event. Neither PRR_{max} nor HRR_{max} can be fairly compared between the cases presented in this work because the combustion phasing varies. However, the observation of multi-stage combustion is a good indicator of a reduction in PRR_{max} compared to HCCI (single-stage combustion) at constant combustion phasing.

It can be seen from Figs. 6 and 7 that PFS results in multi-stage combustion for P_{in} = 2 bar and that the combustion phasing advances with PFS compared to HCCI. Conversely, it can be seen in Figs. 8 and 9 that PFS does not lead to multi-stage combustion at P_{in} = 1 bar and that the combustion phasing is delayed using PFS at P_{in} = 1 bar compared to HCCI combustion. These observations are consistent with those from [5] in that PFS with gasoline results in multi-stage combustion at P_{in} = 2 bar and single-stage combustion at P_{in} = 1 bar. The observed increase in

LTHR with increased P_{in} is consistent with observations in [7].

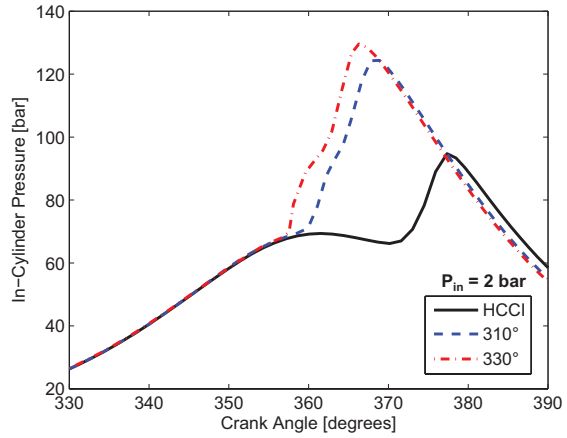

Figure 6: In-cylinder pressure for HCCI and PFS modes at 2 bar intake pressure (T_{in} = 370 K).

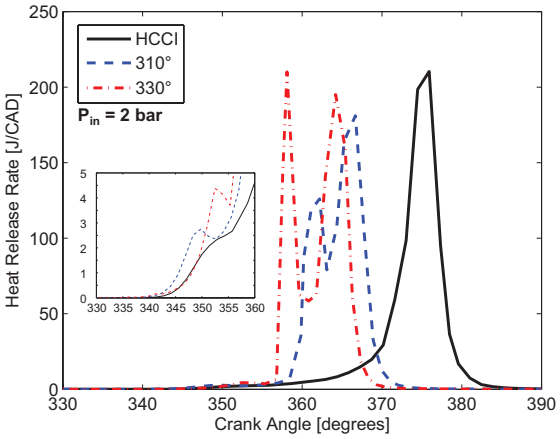

Figure 7: Heat release rate from chemical reactions for HCCI and PFS modes at 2 bar intake pressure (T_{in} = 370 K). The LTHR range is shown (inset).

The influence of the temperature distribution of the ϕ stratification on auto-ignition delay explains the observation of multi-stage combustion for PFS at P_{in} = 2 bar and single-stage combustion at P_{in} = 1 bar. The temperature versus ϕ just after the LTHR range (355 CAD) and the simulated auto-ignition delay times from SENKIN versus ϕ are presented in Figs. 10 and 11 for SOI = 310 CAD and intake pressures of P_{in} = 2 bar and P_{in} = 1 bar, respectively. The auto-ignition delay calculations were performed using the temperature, pressure, and composition at each grid point for grid points with temperature greater than 600 K. At P_{in} = 2 bar, all ϕ regions ($0.3 \leq \phi \leq 0.78$) are approximately the same temperature which results in the auto-ignition delay being shorter for richer regions. As such, the rich regions ignite first followed by the lean regions and multi-stage combustion is observed. At P_{in} = 1 bar, the richer regions are colder than the lean regions ($0.3 \leq \phi \leq 0.75$) due to evaporative cooling from the liquid fuel spray. This temperature distribution offsets the difference in ignition delay time between the lean and rich regions, resulting in single-stage combustion. The increased LTHR from the richer zones at boosted conditions (Fig. 7) leads to thermal equilibration among the ϕ zones such that there is sufficient difference in the auto-ignition delay times between the lean and rich regions for staged combustion to be observed.

The combustion phasing advances using PFS compared to HCCI at P_{in} = 2 bar because the richer zones are more reactive than the leaner zones. The combustion is further advanced with SOI = 330 CAD compared to SOI = 310 CAD because the increased mixture stratification ($0.3 \leq \phi \leq 1.37$) results in greater LTHR. The greater LTHR increases the temperature of the richest zones above that of the lean zones, resulting in even earlier auto-ignition. The combustion phasing retards using PFS compared to HCCI at P_{in} = 1 bar due to evaporative cooling from the liquid fuel spray and the absence of LTHR. The temperature difference between the leanest and richest zones is about the same for SOI = 310 CAD and SOI = 330 CAD, however, the combustion phasing advances with SOI = 330 CAD compared to SOI = 310 CAD because the increased mixture stratification for SOI = 330 CAD ($0.3 \leq \phi \leq 1.31$) results in slightly earlier auto-ignition of the richest zones.

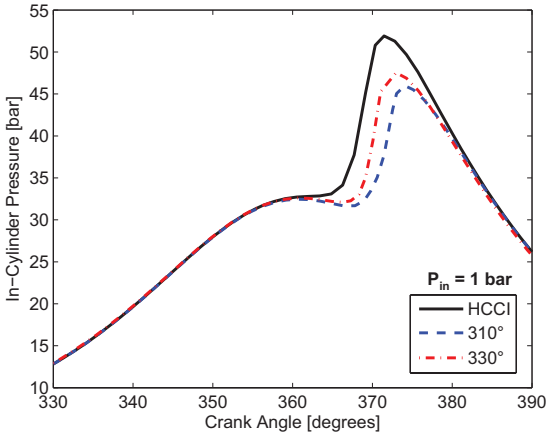

Figure 8: In-cylinder pressure for HCCI and PFS modes at 1 bar intake pressure (T_{in} = 420 K).

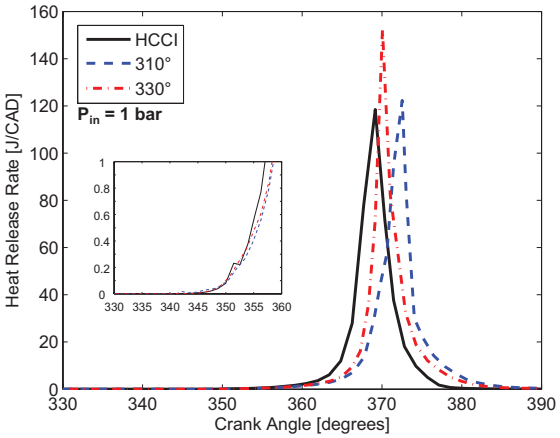

Figure 9: Heat release rate from chemical reactions for HCCI and PFS modes at 1 bar intake pressure (T_{in} = 420 K). The LTHR range is shown (inset).

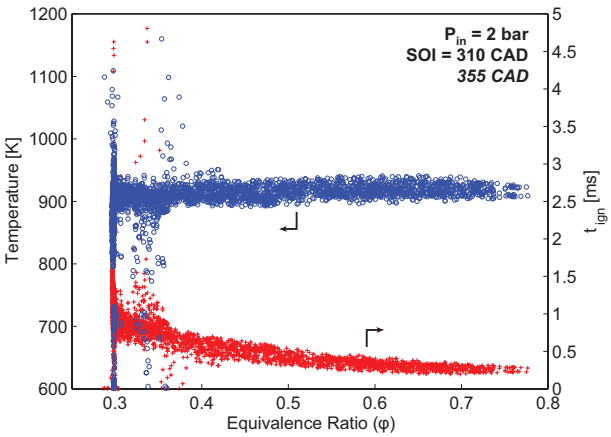

Figure 10: Temperature distribution and ignition delay times of ϕ stratification just after the LTHR range (355 CAD) for PFS with SOI = 310 CAD and P_{in} = 2 bar (T_{in} = 370 K).

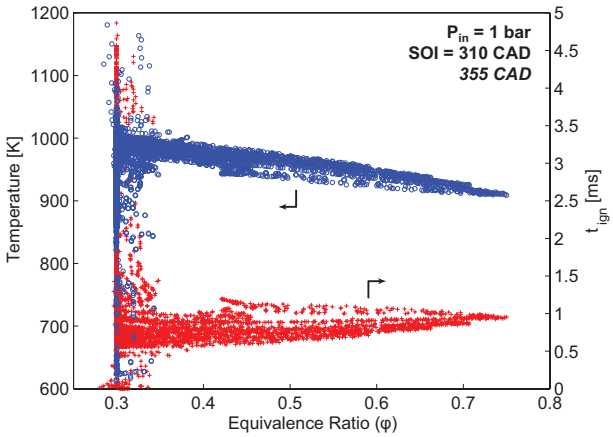

Figure 11: Temperature distribution and ignition delay times of ϕ stratification just after the LTHR range (355 CAD) for PFS with SOI = 310 CAD and P_{in} = 1 bar (T_{in} = 420 K).

4.2 PRF73

Simulations were performed for HCCI and PFS engine operation at ambient intake conditions. HCCI operation was accomplished using an equivalence ratio of ϕ = 0.36 with 4.7% EGR determined using a single zone well-mixed reactor code. PFS operation was accomplished using a homogenous mixture of ϕ = 0.30 (6.9% EGR) with SOI = 310 CAD or 330 CAD to achieve a global ϕ = 0.36 (17% DI). For these simulations, T_{in} = 420 K such that the earliest combustion phasing was near TDC.

The in-cylinder pressure and HRR from chemical reactions determined from simulations are presented in Figs. 12 and 13 for P_{in} = 1 bar. The inset of Fig. 13 highlights the LTHR range. It can be seen in Fig. 12 that SOI = 310 CAD results in a slightly delayed combustion phasing compared to HCCI and that the combustion phasing is advanced towards TDC for SOI = 330 CAD compared to HCCI. HCCI and PFS with SOI = 310 CAD exhibit very similar single-stage HRR profiles while PFS with SOI = 330 CAD exhibits multi-stage combustion and increased LTHR compared to HCCI. These observations are consistent with observations in [6] of multi-stage combustion at P_{in} = 1 bar with 13% DI for SOI = 325 CAD or later. In [6], a higher ϕ was used and LTHR was observed for HCCI and PFS combustion modes. The absence of LTHR for HCCI and PFS with SOI = 310 CAD may be due to the leaner ϕ used in the simulations.

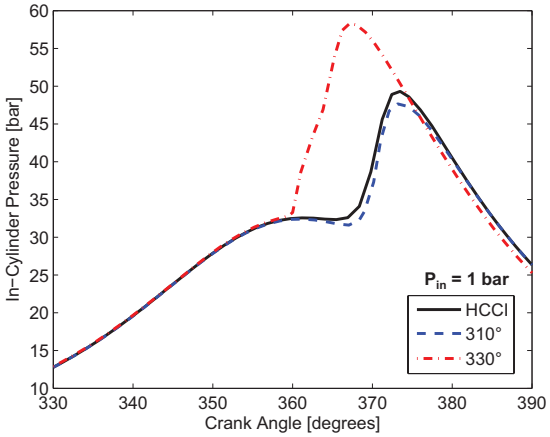

Figure 12: In-cylinder pressure for HCCI and PFS modes at 1 bar intake pressure (T_{in} = 420 K).

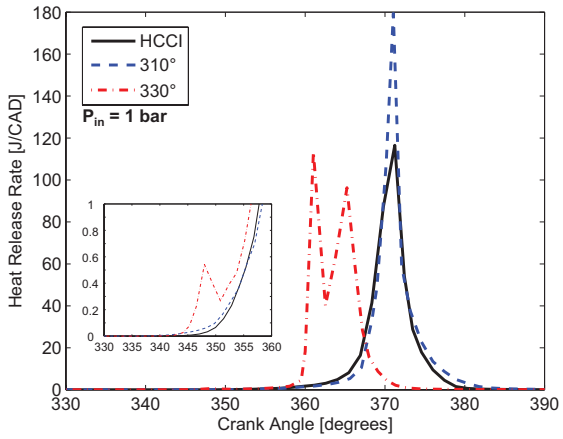

Figure 13: Heat release rate from chemical reactions for HCCI and PFS modes at 1 bar intake pressure (T_{in} = 420 K). The LTHR range is shown (inset).

Similarly to gasoline, the observation of single- or multi-stage combustion can be explained by considering the temperature distribution of the ϕ stratification just after the LTHR range (355 CAD) and the associated auto-ignition delay times, presented in Fig. 14 for SOI = 330 CAD and Fig. 15 for SOI = 310 CAD. For SOI = 330 CAD, the mixture is not quite temperature uniform, but the high degree of stratification ($0.3 \leq \phi \leq 1.34$) leads to shorter ignition delay times for the richest regions compared to the leaner regions, which results in multi-stage combustion. For SOI = 310 CAD, there is less mixture stratification ($0.3 \leq \phi \leq 0.74$) and a higher degree of temperature stratification. The temperature distribution of the mixture stratification causes all ϕ regions to have

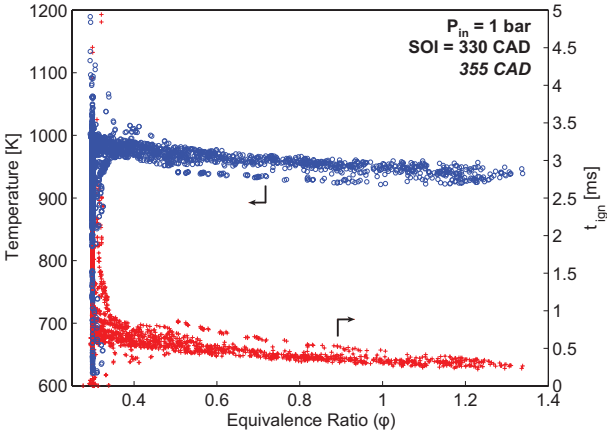

Figure 14: Temperature distribution and ignition delay times of ϕ stratification just after the LTHR range (355 CAD) for PFS with SOI = 330 CAD and P_{in} = 1 bar (T_{in} = 420 K).

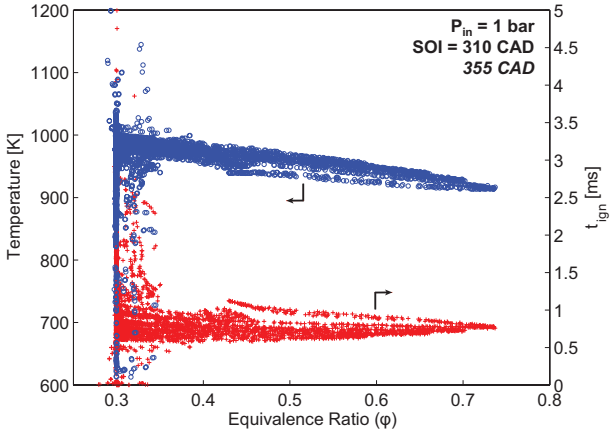

Figure 15: Temperature distribution and ignition delay times of ϕ stratification just after the LTHR range (355 CAD) for PFS with SOI = 310 CAD and P_{in} = 1 bar (T_{in} = 420 K).

approximately the same ignition delay time, leading to single-stage combustion.

5 Conclusions

A 96-species reduced mechanism for a 4-component gasoline surrogate has been developed from a 312-species skeletal mechanism given in Mehl, et al. (2011). Simulations of Partial Fuel Stratification (PFS), a strategy for reducing the maximum pressure rise rate in compression-ignition engines using fuel stratification, have been performed using the reduced mechanism with a modified version of KIVA-3V that computes chemistry using CHEMKIN. Simulations were performed using a CFR engine of compression ratio CR = 14:1. Predictions of low temperature heat release (LTHR), pressure-boost effects, and the behavior of realistic fuels using the reduced mechanism are consistent with experimental observations. The temperature distribution of the mixture stratification dictates whether single-stage or multi-stage combustion is observed. PFS is successful for gasoline at boosted conditions because the greater LTHR leads to thermal equilibration among the different ϕ regions such that the richer regions auto-ignite prior to the lean regions. For gasoline at ambient intake conditions, thermal stratification offsets the differences in ignition delay among the ϕ regions, resulting in single-stage combustion. Conversely, PFS results in multi-stage combustion for PRF73 at ambient intake conditions for sufficiently late injection timing where LTHR is observed.

Acknowledgments

This work at the University of California-Berkeley was partially supported by the University of Michigan, Award No. 3001397038, through a cooperative agreement with the U.S. Department of Energy entitled “A University Consortium on High Pressure Lean Combustion (HPLC) for Ef-

ficient and Clean ICE". The authors would also like to thank Gregory Chin for developing the computational grid of the CFR engine.

References

[1] Xingcai Lu, Dong Han, and Zhen Huang. *Progress in Energy and Combustion Science*, 37 (2011) 741 – 783.

[2] John E. Dec. *Proceedings of the Combustion Institute*, 32 (2009) 2727 – 2742.

[3] J. Dec, W. Hwang, and M. Sjöberg. *SAE Technical Paper*, (2006) .

[4] John E. Dec and Wontae Hwang. *SAE International Journal of Engines*, 2 (2009) 421–438.

[5] J. Dec, Y. Yang, and N. Dronniou. *SAE Int. J. Engines*, 4 (2011) 1169 – 1189.

[6] Yi Yang, John E. Dec, Nicolas Dronniou, and Magnus Sjöberg. *Proceedings of the Combustion Institute*, 33 (2011) 3047 – 3055.

[7] Y. Yang, J. Dec, N. Dronniou, and W. Cannella. *SAE Int. J. Engines*, 5 (2012) 1075–1088.

[8] D. Dahl and I. Denbratt. *International Journal of Engine Research*, 12 (2011) 58 – 68.

[9] Junjun Ma, Xingcai Lü, Libin Ji, and Zhen Huang. *Energy & Fuels*, 22 (2008) 954–960.

[10] S L Kokjohn, R M Hanson, D A Splitter, and R D Reitz. *International Journal of Engine Research*, 12 (2011) 209–226.

[11] J. Abraham. *International Journal of Automotive Technology*, 12 (2011) 721–732.

[12] Zhaolei Zheng, Mingfa Yao, and Weilong Wu. *International Journal of Green Energy*, 7 (2010) 498–515.

[13] Zhaolei Zheng and Mingfa Yao. *Fuel*, 88 (2009) 354 – 365.

[14] Wontae Hwang, John Dec, and Magnus Sjöberg. *Combustion and Flame*, 154 (2008) 387 – 409.

[15] Magnus Sjöberg and John E. Dec. *Proceedings of the Combustion Institute*, 31 (2007) 2895 – 2902.

[16] M. Mehl, J. Y. Chen, W. J. Pitz, S. M. Sarathy, and C. K. Westbrook. *Energy & Fuels*, 25 (2011) 5215–5223.

[17] J.-Y. Chen. *Trans. Aeronaut. Astronaut. Soc. China*, 33 (2001) 59–67.

[18] Marco Mehl, William J. Pitz, Charles K. Westbrook, and Henry J. Curran. *Proceedings of the Combustion Institute*, 33 (2011) 193 – 200.

[19] Robert J. Kee, Fran M. Rupley, Ellen Meeks, and James A. Miller. Chemkin-iii: A fortran chemical kinetics package for the analysis of gas-phase chemical and plasma kinetics. Technical report, Sandia National Laboratories, May 1996.

[20] B.M. Gauthier, D.F. Davidson, and R.K. Hanson. *Combustion and Flame*, 139 (2004) 300 – 311.

[21] S. Jerzembeck, N. Peters, P. Pepiot-Desjardins, and H. Pitsch. *Combustion and Flame*, 156 (2009) 292–301.

[22] Guohong Tian, Ritchie Daniel, Haiying Li, Hongming Xu, Shijing Shuai, and Paul Richards. *Energy & Fuels*, 24 (2010) 3898–3905.

[23] Anthony A. Amsden. Kiva3v: A block structured kiva program for engines with vertical or canted valves. Technical report, Los Alamos National Laboratory, July 1997.

[24] M. Patterson and R. Reitz. *SAE Technical Paper*, 980131 (1998) .

Appendix

Laminar flame speeds calculated using CHEMKIN with the reduced mechanism are compared to experimental data in Figs. 16 and 17. Figure 16 compares computed laminar flame speeds at 373 K and various pressures with data from [21]. Figure 17 compares computed laminar flame speeds at 1 bar and various temperatures with data from [22]. The experimental laminar flame speed data exhibits some scatter, but overall there is agreement with the calculated laminar flame speeds.

Laminar flame speeds calculated using CHEMKIN with the reduced mechanism are compared to laminar flame speeds calculated using the detailed mechanism (results from [16]) in Figs. 18 and 19. Figure 18 compares computed laminar flame speeds at 373 K and various pressures. There is good agreement between the reduced and detailed mechanisms near stoichiometric conditions, with the reduced mechanism slightly over predicting the laminar flame speed. For ϕ less than about 0.85, the reduced mechanism under-predicts the laminar flame speed compared to the detailed mechanism. The difference between the reduced and detailed mechanism becomes larger as ϕ becomes smaller. Figure 19 compares computed laminar flame speeds at 1 bar and various temperatures. The laminar flame speeds are over-predicted using the reduced mechanism compared to the detailed mechanism at 1 bar for the ϕ range presented. However, the reduced chemistry was developed for engine applications where the pressures at which reactions occur are much greater than 1 bar.

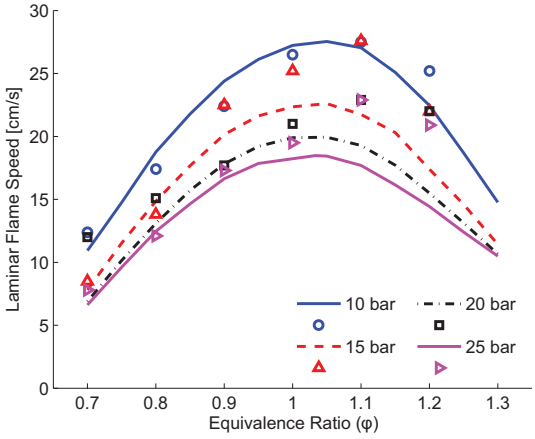

Figure 16: Laminar flame speeds at 373 K and various pressures from simulation and experiments (from [21]).

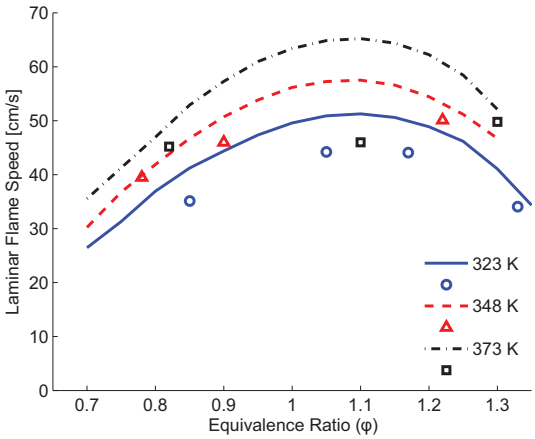

Figure 17: Laminar flame speeds at 1 bar and various temperatures from simulation and experiments (from [22]).

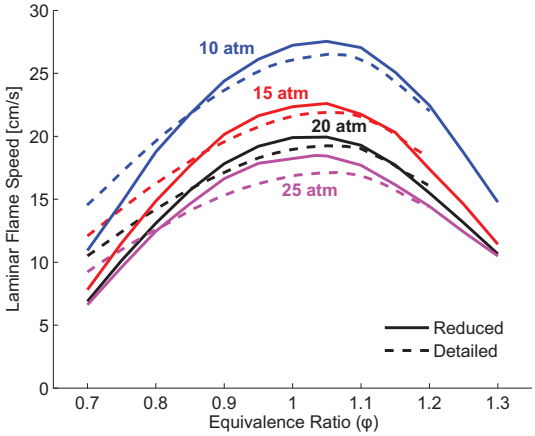

Figure 18: Laminar flame speeds at 373 K and various pressures from simulation for the reduced and detailed (data from [16]) mechanisms.

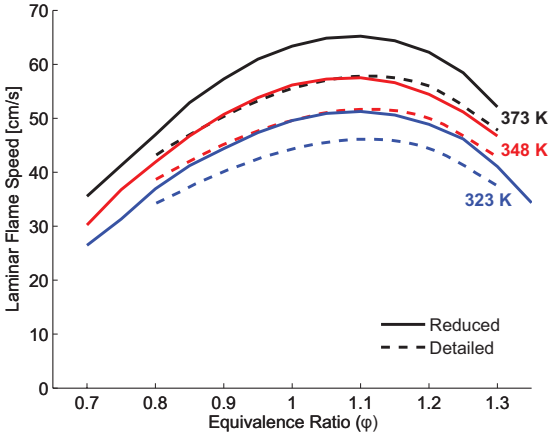

Figure 19: Laminar flame speeds at 1 bar and various temperatures from simulation for the reduced and detailed (data from [16]) mechanisms.